IEEE Access
Multidisciplinary | Rapid Review | Open Access Journal

Received December 10, 2020, accepted December 23, 2020, date of publication December 28, 2020,
date of current version January 8, 2021.

Digital Object Identifier 10.1109/ACCESS.2020.3047696

Butler Matrix Based Beamforming Networks For Phased Array Antenna Systems: A Comprehensive Review and Future Directions For 5G Applications

ARSHAD KARIMBU VALLAPPIL[1], MOHAMAD KAMAL A. RAHIM[1], (Senior Member, IEEE), BILAL A. KHAWAJA[2,3], (Senior Member, IEEE), NOOR ASNIZA MURAD[1], (Senior Member, IEEE), AND MOHAMMED GAJIBO MUSTAPHA[1]

[1]Advance RF and Microwave Research Group (ARFMRG), School of Electrical Engineering, Faculty of Engineering, Universiti Teknologi Malaysia, UTM Johor Bahru, Johor 81310, Malaysia
[2]Department of Electrical Engineering, Faculty of Engineering, Islamic University of Madinah, Madinah 41411, Saudi Arabia
[3]Department of Electronics and Power Engineering, PN-Engineering College, National University of Sciences and Technology, Karachi 75104, Pakistan

Corresponding authors: Arshad Karimbu Vallappil (kvarshad2@graduate.utm.my) and Bilal A. Khawaja (7166@iu.edu.sa)

This work was supported in part by the Ministry of Higher Education, in part by the Research Management Centre, School of Postgraduate Studies, and in part by the School of Electrical Engineering, Universiti Teknologi Malaysia, Johor Bahru, under Grant 04G72/09G19/06G15.

ABSTRACT Due to the rapid development of wireless communication technologies, the number of wireless users are radically increasing. Currently, ∼23 billion wireless devices are connected to the internet, and these numbers are expected to increase manifolds in the years to come. The technology growth of the fifth-generation (5G) wireless systems will be needed to meet this high demand of the network. 5G wireless systems offer data-rates of up to 10Gbps, 1-ms latency, and reduced power consumption. It is a known fact that 5G wireless systems will be exploiting beyond the presently used 3 GHz microwave and millimetre-wave (mm-wave) frequency bands. This is the primary driver in the development of the 5G wireless system. Multi-beam Phased array antenna (PAA) systems are typically used in the deployment of 5G systems for high-gain and directionality. In current 5G and future Beyond 5G (B5G) antenna array systems, beamforming networks (BFNs) such as the Butler Matrix (BM) will play a key role in achieving multi-beam characteristics. So, this paper presents an extensive review of the BM based BFNs, and discusses which type of BM will be suitable for the phased array antenna (PAA) systems in the upcoming 5G and next-generation of B5G wireless systems. Moreover, this paper also summarizes the different types of BM designs based on the number of layers. The BMs are classified into the bi-layer, tri-layer, and four-layer structures. It includes different techniques that have been used to solve the problem of crossing, narrow bandwidth, and size reduction of the BM. From the previous studies, it is found that most of the past research work was performed using the bi-layer BM system, whereas the difficult geometries like tri- and four-layer BM are avoided due to their complex fabrication process. It is also found in this paper that the metamaterial (MTM) based bi-layer BM achieves low insertion-loss and phase-error, excellent bandwidth and compact size, and good S-parameter performance, which makes them an ideal BFN candidate for the upcoming 5G and next-generation B5G systems.

INDEX TERMS Butler matrix (BM), metamaterial (MTM), 5G, beyond 5G (B5G), beamforming network (BFN), phased array antenna (PAA) systems.

I. INTRODUCTION

Multi-beam antennas have been at the forefront of modern wireless communications for the last two decades [1]–[7]. Typically, the phased array antenna (PAA) systems use multi-beam antennas because the direction of its beams often depends on the phase, and the variations between them [8]. Multi-beam and beam-scanning antennas play a key role in modern wireless communication systems to get the desired output. In many applications, such as WLANs [9], base-stations [10], satellite communications [10], and even automotive radars [6], the multi-beam antennas concept has

The associate editor coordinating the review of this manuscript and approving it for publication was Derek Abbott.

already been implemented, in order to achieve wide-angle coverage. The PAA system with multi-beam antennas is considered an ideal candidate for the 5G wireless systems and mobile terminals [8], [11], [12] to achieve both wide coverage and high-gain. As stated in [11] and [12], the PAA system is used to achieve multiple beams and decent coverage performance, but expensive transmitter/receiver (T/R) modules and the complexity of the PAA hardware design are some of the significant factors that needs to be taken into account. For practical usage and large-scale deployment, it is essential that the feed networks for the PAA systems are low in profile and fabrication cost.

In the PAA system, the main beam is steered by appropriately changing the radiating elements phase and amplitude using beamforming networks (BFNs). So, most research has been focused on BFNs [13]–[16] as it is the most critical part of the system. BFNs for multi-beam antennas are of great interest due to their accuracy and versatility in a wide variety of applications, including terrestrial and space telecommunications [15] and 5G communication systems [16].

The BFNs can be classified into two different categories, which are Digital BFNs, and RF BFNs [17]. Digital BFN is usually related to the adaptive array system, while RF BFN is typically used in the multi-beam antenna system. The benefit of digital beamformers is that they have zero phase-error, adjustable amplitude tapering, and an infinite number of scanning steps. Although, they do suffer from receiver channel imbalances, analog-to-digital (A/D) offset-errors, and frequency-dependent errors [18]. The RF BFNs, on the other hand, are further classified into two sub-categories which are, Lens-based beamformer (Rotman lens) [18] and circuit-based beamformer [19]. The Rotman lens (RL) is an attractive BFN due to its reliability, simplicity, and wide-angle scanning capabilities. As the RL is also a true time delay (TTD) device, it works for possible extreme wide-band operation [19]–[23]. The mathematical framework for the ground calculation of the RL design is referenced to the paper of Simon [24]. Whereas, Blass [25], Nolen [26], and BM [27] are considered the most commonly used circuit-based BFNs. Circuit-based BFNs are constructed using basic building blocks, such as directional couplers, phase-shifters, and crossovers. Due to their simple fabrication process and low-cost, the most commonly used BFNs recently are the BM [28], which is used for feeding the PAA system. Fig. 1(a) shows the flow-chart for the different types of commonly used RF beamformers, whereas Fig. 1(b) shows the advantages and disadvantages of BM based BFNs and Fig. 1(c) shows the block diagram of the BM, respectively.

A. REQUIREMENTS OF 5G AND B5G BFNS

In the 5G wireless systems, both microwave (3-30GHz) and mm-wave (30-300GHz) frequency bands are expected to be deployed in the year 2020 [29]. It is also envisioned that multi-beam antenna technologies such as beamforming are expected to play a key role in 5G and B5G systems. The particular features and difficulties related to these frequency bands have sparked a study of the architecture and efficiency tradeoffs associated with current multi-antenna technologies to determine the ideal method for implementing BFN in 5G networks. Below are the main design goals for the new 5G system model. These targets are the theoretical maxima that could be supported under ideal conditions by the system [30].

1) Support bandwidths up to 0.5-1 GHz
2) Compact PAA system

The mm-Wave 5G signals severely suffer from multi-path fading, path-loss, and atmospheric absorption. This problem can be solved by using a large number of antennas with the BFN network in the 5G wireless system transceiver [31], [32]. So, the BFN based PAA system is fundamentally required for the 5G and B5G transceiver architecture to improve the coverage with high directionality [33]. The analog BFN can be divided into two structures. One is based on a variable phase-shifter (VPS), and the other one is a fixed passive beamformer like a lens-based or BM based structure. The VPS is further sub-divided into active and passive structures, respectively. Both techniques have limitations such as high power consumption for the active VPS and high insertion-loss for the passive VPS [34]. The appropriate solution is the use of BM for the 5G PAA system with the following characteristics [35]:

- In the signal path, there should not be any active components.
- Power consumption and insertion-loss should be low.
- BM should provide a fixed radiation pattern with different phases.
- BM should be of compact size and provide enhanced bandwidth.

The 5G applications, such as enhanced mobile broadband (eMBB) and massive Internet of things (M-IoT), need a large number of transmitting and receiving antennas. So, the design of BFN based PAA systems should also be compact, low in profile, and ideal in fabrication cost for practical use and large scale deployment.

B. CONTRIBUTIONS AND ORGANIZATION OF THIS ARTICLE

In this article, our contributions are as follows: Recent literature studies [3], [36], [37] have discussed multi-beam antennas based on beamforming circuits, optical components, and different phase switching methods, in general. Although, they failed to discuss in detail the different types of beamforming circuits based on the BM number of layers. Our main aim in this paper is to provide a comprehensive literature review on the classification of BFNs based on BM. Then, this paper will briefly discuss and compare the results of various types of BM based on different techniques. This paper will also discuss the challenges and requirements of 5G and B5G wireless networks and their BFNs. Finally, this paper provides the selection criteria of BM based BFN suitable for 5G and B5G technologies. These findings will give future directions to the research fraternity working in this area and help them make

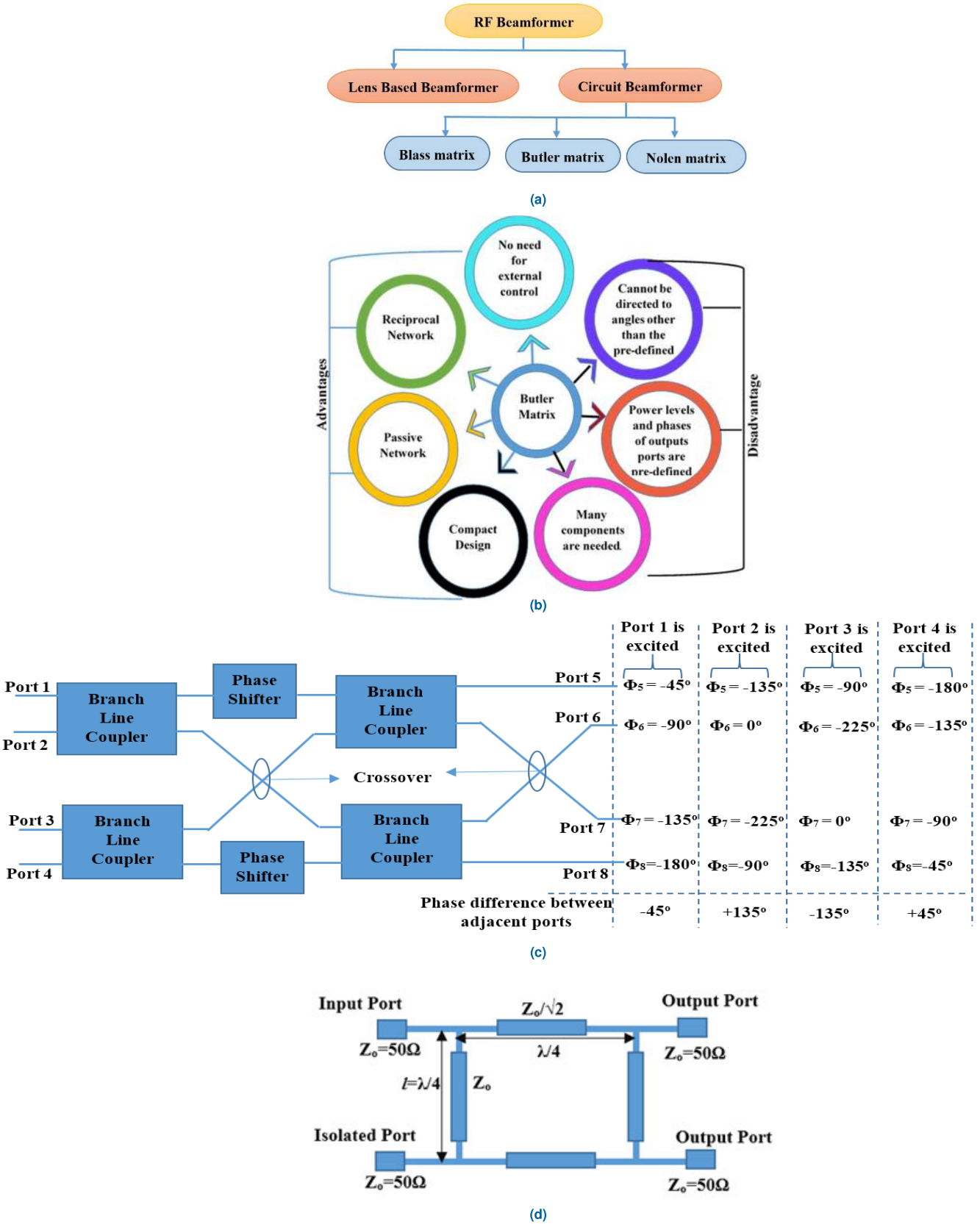

FIGURE 1. (a) Flow-chart of RF BFNs (b) Advantages and disadvantages of BM (c) Block Diagram of the BM (d) 90° 3dB Branch Line Coupler Structure.

better decisions for the selection of BFN with respect to their applications and PAA systems.

The rest of the paper is structured as follows; Section II discusses the classification of BM and presents a detailed literature review of different types of BM based on the number of substrate and ground layer positions. In Section II, approximately 38 papers based on bi-layer BM, 12 papers based on tri-layer BM, and 4 papers based on four-layer BM were discussed. The discussion was focused on the summary of BM based on layers, operating frequency, performance parameters like phase-error, insertion-loss, isolation-loss, and return-loss, etc, and which technique achieved both bandwidth improvement and size reduction. Then, Section III gives a detailed summary of the paper where the most important findings of the paper are discussed, and finally, Section IV draws the conclusion. The paper organization in pictorial form is shown in Fig. 2.

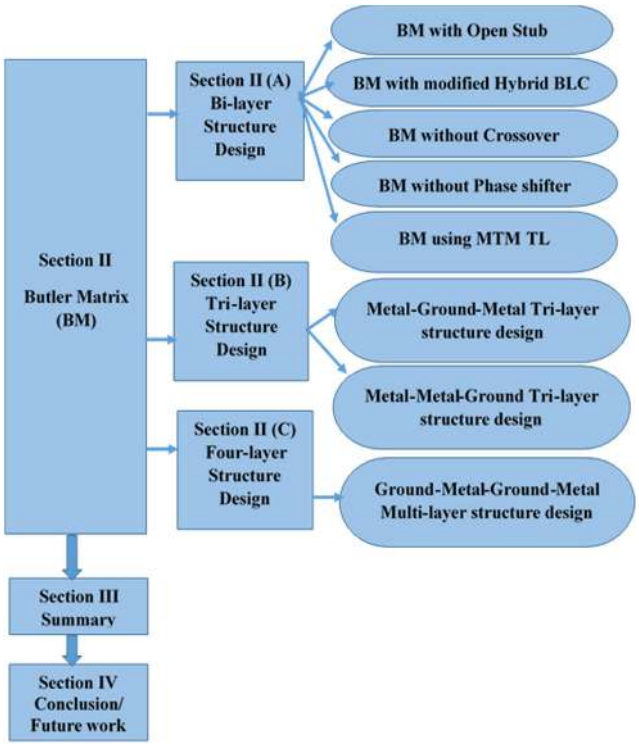

FIGURE 2. The paper taxonomy.

II. BUTLER MATRIX

The BM is a BFN that is used to feed the multiple antenna array element. The BM has 'N' input ports connected to the main transceiver to get a signal and 'N' output ports connected to the antenna elements of the PAA system. With a progressive phase difference between the output ports, the BM feeds the signal from the transceiver to the antenna elements so that the beamforming operation can be performed, and the signal can be transmitted in different directions. The beam direction is controlled by applying a signal to the specific input port.

A $N\times N$ BM is a passive BFN consisting of $(N/2)^*log_2N$ branch-line coupler (BLCs), $N/2^*log_2(N-1)$ phase-shifters, and 0dB crossovers. Fig. 1(c) shows the 4×4 BM, which consists of four 90° BLCs, two 45° phase-shifter, and two crossovers. Ports 1-4 are considered as input ports, and Ports 5-8 are considered as output ports, respectively. In conventional BM [27], when a signal is fed to ports 1, 2, 3, 4, the phase difference generated between the adjacent output ports are $-45°$, $+135°$, $-135°$, $+45°$, respectively. For example, when the signal is fed to port 1, the phase difference will be $-45°$ between port 6 and port 5, $-45°$ between port 7 and port 6, and $-45°$ between port 8 and port 7, respectively. Similarly, when port 2 is excited, the phase difference will be $+135°$ between port 6 and port 5, $+135°$ between port 7 and port 6, and $+135°$ between port 8 and port 7, respectively. The similar behavior can be observed for port-3 and port-4 excitation, and their respective phase difference between the adjacent output ports will be $-135°$ and $+45°$. The details about the phase difference between the adjacent port of BM is shown in Fig.1(c). The 90° BLCs have two input ports, and two outputs with the phase difference between the output ports being 90°. The BLC is constructed using two horizontal and two vertical microstrip-lines of length $\lambda/4$, having a characteristic impedance of $Z_0/\sqrt{2}$ and Z_0, respectively. The structure of the BLC is shown in Fig. 1(d). The crossover is implemented by cascading two BLCs. The use of crossover is to pass the signal to the second stage of the coupler with 0dB insertion-loss and high isolation-loss. The phase-shifter is implemented based on the microstrip-line of length $L=(\varphi^*\lambda)/2\pi$, where φ represents the required phase shift [27]. The performance parameters such as bandwidth, return-loss, isolation-loss, insertion-loss, and the phase difference between the output ports depend on the individual components of the BM. The practical average insertion-loss for 4×4, 8×8, and 16×16 BM are -7dB, -10dB, -13dB, respectively [38], [39].

The number of metallic layers used in the structure is the major classification used to categorize the research performed for the BM network. This analysis involves three groups:

1. Bi-layer Structure
2. Tri-layer Structure
3. Four-layer Structure

The classic BM design is a bi-layer structure network. The bi-layers consist of a metallic conductive layer and a ground layer.

A. BI-LAYER STRUCTURE DESIGN

The idea of BM network was first coined by Butler and Lowe [27] in 1961. A typical BM is a bi-layer structure that consists of three key components: couplers, crossovers, and phase-shifters, respectively. Due to the hybrid couplers, crossover, and phase-shifters employed in the BM design, the conventional BM is large in size and has bandwidth limitation. This can be improved by introducing a novel design for BM components. The second issue with the conventional design is crossing. To solve this problem, many innovative

ideas and novel designs were proposed by a number of researchers [40]–[81]. Because of the crossover problem, researchers started to create new geometry for the BM, where they could reduce the number of required crossings. Some new crossover designs achieved greater bandwidth, whereas other designs have managed to avoid the use of crossovers entirely [62]–[68].

So, this section will discuss five different types of bi-layer BM structures which were used to improve the bandwidth and miniaturize the conventional BM design. The structures are:

1. BM with Open-Stub
2. BM with modified Hybrid BLC (HBLC)
3. BM without crossover
4. BM without Phase-shifter
5. BM using MTM transmission-line (TL)

1) BM WITH OPEN-STUB

In [40], the use of 45° and 90° phase-shifters and four BLCs miniaturized with the use of open-stubs in each TL facilitates a 42.68% reduction in size relative to a conventional BM. The size reduction was due to the removal of crossover and miniaturization of BLC. A compact broadband BM with a flat coupling [41] was achieved through novel disk hybrids, and improved phase-shifters with an open-stub, which was fabricated using a 1.5mm thick dielectric substrate with permittivity (ε_r) of 2.65. The overall structure was compact, had an excellent flat coupling and return-loss with a bandwidth of 23.8%. The article [42] presented the design and fabrication of a 4 × 4 BM for feeding a smart PAA system, as shown in Fig. 3. The design used open-stubs of half-wavelength with a width of 0.5mm. This compact structure eliminated the crossovers that resulted in additional loss and impedance mismatch. When compared with the conventional BM, the circuit size was reduced to 71%.

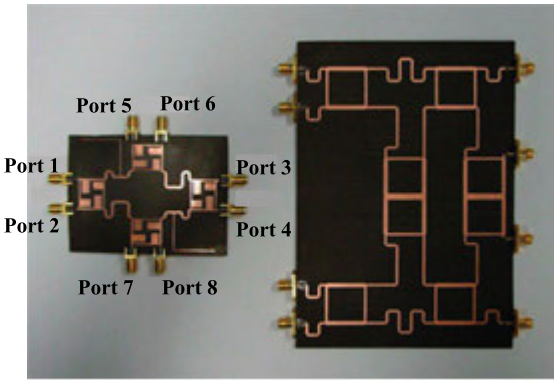

FIGURE 3. Prototype of fabricated BM with open stub and conventional BM [42].

A simple planar 4 × 4 BM design was presented in [43]; it consisted of half-wavelength open-stubs to enhance the phase difference between the output ports. The proposed BM was fabricated using a substrate of dielectric constant 3.05 and 1.52mm thickness. The author inserted half-wavelength open-stubs on the opposite side of the eighth-wavelength delay lines. Another configuration of miniaturized 4 × 4 BM by using novel reduced size BLC was reported in [44]. The BLC size reduction was achieved by inserting twelve capacitive plates and eight two-step stubs [44]. Eight two-step stubs consisted of 4 '+' shaped and 4 'L' shaped stubs inserted at the center and the corner of the horizontal and vertical TL of BLCs, respectively. The twelve capacitive plates consisted of 4 square-shaped and 8 triangular-shaped microstrip structures. The four square-shaped capacitive plates were attached to the L-shaped stub, and eight triangular-shaped capacitive plates were attached to the + shaped stub. This resulted in a size reduction of approximately 80% as compared to conventional BM without changing the performance. In [45], a cascaded BM operating at 2.45GHz was designed. In this design, the size reduction was achieved by using eight two-step stubs in the BLC and cascading the BM using Wilkinson power divider. The area of BLC had also been reduced to 30%. Another four-element planar BM design using two-section BLC was discussed in [46]. A 90° short stub was inserted across the two-section branch-line hybrids to improve broadband performance. In [47], a miniaturized BM network was proposed and experimentally verified with the help of a microstrip antenna array. The stub-loaded TLs were introduced to miniaturize the BM network. The size of the BM was reduced to 55% as compared to conventional BM. A 90° short stub was inserted across the two-section branch-line hybrids of BM in [46], which improved the bandwidth by 16.7%. In [48], a planar compact 4 × 4 BM, which operated over a frequency range of 4.5-5.5GHz, was developed using lumped elements and multiple U-shaped Schiffman phase-shifter. In the proposed design, the lumped-distributed elements meant an open-stub using a microstrip-line. In [49], researchers reported a 16 × 16 BM consisting of a shunt open-and-short stub based Schiffman phase-shifter, 90° directional coupler, and a crossover. The proposed BM was operating over a frequency range of 9-11GHz with reduced transmission-loss.

In this section, 10 research papers using stubs in the BM design and without crossover were discussed in detail. From the comparison presented in Table 1, it can be concluded that most of the researchers concentrated their efforts on the development of compact BM design. Although, researchers in articles [42], [44], and [48] demonstrated both compact and bandwidth improved BM designs as compared to other research articles and also gave better results in terms of performance parameters. The main challenge for the 5G BFN is to design accurate BM with low insertion-loss [50]. From the analysis of BM design based on the open-stub, it is understood that all of them have high insertion-loss, as shown in Table 1. So, this high insertion-loss will not divide the power equally from all output ports, which will affect the transmitter efficiency and cause severe degradation in the noise figure of the receiver [51]. Most of the open-stub based BM analysis was performed below 5GHz, where the insertion-loss is high, and it will be more severe at higher

TABLE 1. Review on BM with open-stub.

Ref. / Year	ε_r , h	f_o (GHz)	Technology	Insertion-loss / Phase-error	Bandwidth Improvement / Size reduction	Return-loss / Isolation-loss
[40] / 2017	4.4, 1.59mm	2.5	Inserted open-stubs in each TL and removing crossover	-5.5 to -7.5dB / ±3°	8% / 42.68%	-15dB / -15dB
[41] / 2007	2.65, 1.5mm	4.2	Novel disk hybrids and improved phase-shifter with open-stub and removing crossover	-7.2 ± 0.7dB / ±7°	23.8% / -	<-10dB / <-10dB
[42] / 2007	2.65, 0.5mm	2.4	Open-stubs of half wavelength with a width of 0.5 mm and without crossover	6.45 ± 0.7dB / ±4°	20.8% / 71%	<-10dB / <-20dB
[43] / 2002	3.05, 1.52mm	0.85 - 0.9	Open-stubs inserted on the opposite side the eighth-wavelength delay lines	-6.45 ± 0.25dB / ±2°	6% / 10%	-17dB / -15dB
[44] / 2001	4.4, 0.5mm	1.8	Inserted 12 capacitive plates that has been achieved by 8 two-steps stub	-9.7 to -10dB / ±6°	16.6% / 80%	-49dB / -30dB
[45] / 2010	4.6, 0.8mm	2.45	Eight two-step stubs in the BLC and cascading of the BM using Wilkinson power divider	-7 to -12dB / ±6°	13% / 30%	-14dB / -17dB
[48] / 2011	3.38, 0.813mm	5	Open-stub and multiple U-shape schiffman phase-shifter	-8 dB / ±10°	20% / 50%	-20dB / -20dB
[49] / 2019	2.9, 0.1mm	26-31.4	Shunt open-and-short stub based schiffman phase-shifter	-15 ± 1dB / ±16°	20% / 50%	<-10dB / <-10dB

frequencies [52]. The next issue is the high phase-error / deviation, which also increases at higher frequencies. The only advantage of this technique is the compact size and enhanced bandwidth. So, from this discussion, it can be concluded that this technique is not suitable for 5G BFNs.

2) BM WITH MODIFIED HYBRID BLC(HBLC)

This section presents a detailed discussion about the BM with modified HBLC that includes patch hybrid coupler, BLC with phase difference, and novel HBLC.

In [53], to achieve broadband characteristics, the BM utilized BLCs in two sections and branch crossovers in four sections, as shown in Fig. 4. This technique improved the bandwidth of the BM to 27.08% as compared to the conventional BM. A novel design of a compact 4 × 4 BM was presented in [54]. The compact BM designed by using Lange coupler and crossover reduced the overall size by 80% as compared to conventional BM designed at the same frequency. The Lange crossover added undesired effects, such as increased insertion-loss and mismatched junction. Article [55] presented a 4 × 4 BM and introduced couplers

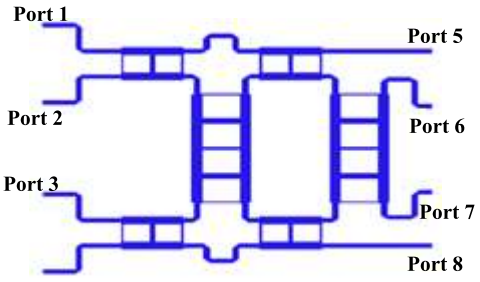

FIGURE 4. The Structure of BM with modified branch-line coupler [53].

with arbitrary phase-differences to replace individual BLCs and phase-shifter in the conventional BM. The bandwidth of the BM was improved by 15% as compared to conventional BM. A high isolation 4 × 4 BM was designed and fabricated on a single-layer PCB substrate, as presented in [56]. It includes four modified hybrid couplers, one crossover, two phase-shifters that provides a frequency range from 1.920GHz to 2.170GHz. In [57], the researchers presented the 4 × 4 BM based on the patch element instead of BM based on the microstrip-line to avoid performance degradation at a higher frequency. The proposed BM consists of couplers with arbitrary phase difference and a novel crossover based on patch element. The proposed BM had an excellent performance that covered high-frequency range between 9GHz and 11GHz with the help of the unique advantages of the patch element.

A wide-band BM based on the four 3-dB cross-slotted patch hybrids with inter-digital coupled-lines loaded at each port, two 45° phase-shifters, and two short ended stubs was presented in [58]. The above BM was designed at 2.65GHz and 12.5GHz, and it achieved bandwidth improvement of 36% compared to the conventional BM. In [59], BM miniaturization was achieved by inserting 45° phase-shifters with short-circuited stubs and cross-slot patch hybrid couplers. This helped reduce the BM size by 56% as compared to conventional BM, and the bandwidth was enhanced by 14%. A BM based on non-uniform BLC was presented in [60] to enhance the bandwidth. For the 4 × 4 BM configuration, the impedance of the BLC series arms was tapered exponentially to achieve a bandwidth of 17% at the center frequency of 9.4GHz. The article [61] presented a single layer 4 × 4 BM based on modified BLC without phase-shifters and crossover. The 45° phase-shifters were removed by designing

TABLE 2. Review on BM with modified HBLC.

Ref. / Year	ε_r , h	f_o (GHz)	Technology	Insertion-loss / Phase-error	Bandwidth Improvement / Size reduction	Return-loss / Isolation-loss
[53] / 2014	4.4, 1.58mm	2.4	BM utilizes BLC in two sections and branch crossover in four sections	-7 ± 1dB / ±4.41°	27.08% / 12%	-35dB / -30dB
[54] / 2018	6.15, 1.27mm	2.45	Lange coupler and Lange crossover is proposed to design BM	-7 ± 1dB / ±4.5°	6% / 80%	<-10dB / <-10dB
[55] / 2016	2.2, 0.787mm	5.8	Hybrid BLCs with arbitrary phase-differences	-7 ± 0.75dB / ±6°	15% / 8%	<-16dB / <-18dB
[56] / 2009	2.55, -	1.92 - 2.17	Four modified wide-band hybrid coupler, one wide-band crossover coupler, and two phase-shifter	6.8 ± 1dB / ±13 °	12.2 / -	-23dB / -26dB
[57] / 2015	2.2, 0.813mm	10	Couplers with arbitrary phase difference and a novel crossover based on patch element are introduced to design BM	-7.3 ± 0.7dB / ±5°	20% / 13%	<-10dB / <-10dB
[58] / 2014	3.66, 0.508mm	2.65 , 12.5	Cross-slotted patch hybrids, two shortened stubs and inter-digital coupled-lines kept at each port	2.65GHz: -6 ± 0.7dB / ±5° 12.5GHz: -8 ± 2 dB / ±9°	36% / -	<-10dB / <-10dB
[59] / 2013	3.66, 0.508mm	2.4	45° phase-shifters with short-circuited stubs and cross-slot patch hybrid couplers	-7 ± 0.7dB / ±5°	14% / 56%	<-10dB / <-10dB
[60] / 2012	2.3, 1.57mm	9.4	Non uninform BLC and crossover	-5 to -10dB / ±7°	22% / -	<-25dB / <-10dB
[61] / 2012	3, 0.25mm	6	Modified BLC with 45° output phase difference	-5 to -9dB / ±5°	37% / -	<-17dB / <-17dB

a modified coupler with an output phase difference of 45°. The proposed BM had a bandwidth of 37% at the center frequency of 6GHz.

In this section, 9 papers that used modified HBLC in the BM were discussed. From Table 2, it can be concluded that most of the articles were focused either bandwidth improvement or reducing the size of BM by modifying the BLC. All the BM designs presented in Table 2 depicts simple geometry, which leads to avoid complex fabrication and cost reduction. Only research articles [58] and [61] have provided bandwidth improvement design as compared to other research articles. In Section I (A), we have already discussed the importance of insertion-loss and phase-error in 5G BFNs. From Table 2, it can be understood that the insertion-loss and phase-error increase proportionally with respect to the frequency. At lower frequency, the insertion-loss value is approximately close to the ideal value of −7dB, but at higher frequency, it reaches −10dB. In [58], a dual-band BM design is presented, which shows that as the frequency changed from 2.65GHz to 12.5GHz, the insertion-loss and phase-error also increases. This will severely degrade the performance of transmitter and receiver efficiency. From all this analysis, it can be concluded that the BM with modified BLC is only applicable for sub 6GHz and not advisable for high frequency mm-wave operation.

3) BM WITHOUT CROSSOVER

As shown in Table 3, in [62], a novel broadband BM was presented using 180° BLC in place of 90° couplers and without crossover. The proposed BM works over the frequency range of 1.6-2.4GHz with an excellent amplitude and phase response. In [63], the paper dealt with the 4 × 4 microstrip BM without any crossing in mm-waves that operated at 40GHz. A 3dB square patch coupler based on BM, which operated at 4GHz, was presented in [64]. The bandwidth of the proposed BM was improved by inserting via hole to wide-band phase-shifter based on a triangular patch. In [65], the BM consisted of two 45° and two 90° couplers, without any crossover. The 45° and 90° couplers were based on a dumb-bell shape and cross slots, respectively. A short strip TL was used to connect the couplers. A novel 4 × 4 BM based on four modified 90° couplers and two-stepped 45° phase-shifters was reported in [66]. The 90° couplers consisted of meandered microstrip-lines and cross slots in the rectangular patch. Article [67] presented a BM without crossover in order to reduce the losses and size. The BM consisted of four 90° couplers and two 45° phase-shifters. The proposed structure operated at 5GHz and 8GHz, respectively. Two 4 × 4 and 8 × 8 BM operated at 2.44GHz and 1.9GHz, respectively, were reported in [68]. In 4 × 4 BM design, diamond, circular, and rectangular-shaped couplers were used.

TABLE 3. Review on BM without crossover.

Ref. / Year	ε_r , h	f_o (GHz)	Technology	Insertion-loss / Phase-error	Bandwidth Improvement / Size reduction	Return-loss / Isolation-loss
[62] / 2011	4.4, 1.6mm	2	Schiffman's phase-shifter and 180° BLC are used to construct 4x4 BM without crossover	-7 ± 1dB / ±7°	40% / -	<-15dB / <-15dB
[63] / 2003	2.94, 0.254mm	40	Without crossover	-7 ± 1dB / ±3°	15% / -	<-17dB / <-15dB
[64] / 2016	3.66, 0.508mm	4	3dB square patch coupler and inserting via hole to wide-band phase-shifter based on triangular patch are used to construct BM	-7 ± 1dB / ±5°	18% / -	-38dB / -20dB
[65] / 2019	2.2, 1.57mm	6	45° and 90° couplers without crossover	6.5 ± 1.5dB / ±3°	14.1% / -	-40dB / -30dB
[66] / 2019	-	32 - 38	Without crossover	-6. ± 1dB / ±4°	-	-60dB / -30dB
[67] / 2014	2.2, 0.787mm	5, 8	90° couplers, 45° phase-shifters, no crossover	5GHz: 7.2 ± 0.5dB / ±5° 8GHz: -8 ± 0.5dB / ±7°	-	-20 dB / -20dB
[68] / 2019	4.35, 1.5mm	2.44	4×4 BM without crossover. Rectangular shaped coupler with smooth microstrip bend to connect with each other	-7 ± 1dB / ± 7°	13.1% / -	<-15dB / <-15dB
[68] / 2019	4.35, 1.5mm	1.9	8×8 BM without crossover	-12 ± 1.5dB / ± 12°	12.1% / -	<-15dB / <-15dB

Out of these designs, they selected the rectangular-shaped 90° coupler without a crossover to fabricate the 4 × 4 and 8 × 8 BM. The four couplers are connected to each other using a smooth microstrip-line bend as shown in Fig. 5.

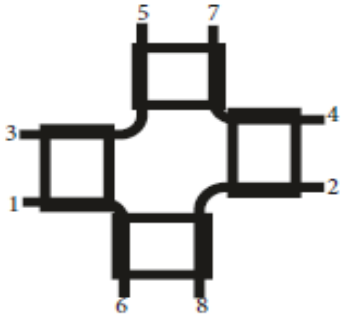

FIGURE 5. Layout of 4 × 4 BM without crossover [68].

In this section, 7 papers based on 4 × 4 BM without crossover and 1 paper on 8 × 8 BM without crossover were discussed. In the discussed papers [62]–[68], the researchers have reported the operating frequencies from 1.9GHz to 12.5GHz. From the review, it was understood that for the 4 × 4 BM design without crossover, the overall size was reduced, and performance parameters like insertion-loss and phase-error were almost close to the ideal value of −7 dB and ±3° to ±7°, respectively. As in the case of 8 × 8 BM [68] design without crossover, the insertion-loss value reached −12 ± 1.5dB with respect to the ideal value of −10dB, and the phase-error value is ±12° at the center frequency of 1.9GHz. So, it means that at the lower frequency itself, the performance parameter is severely degraded for the 8 × 8 BM, and the structure is too complex as compared to the 4 × 4 BM. The mm-wave frequency always suffers from path-loss and penetration loss [33]. So, a large number of antenna and BM networks (for example, 16 × 16, 32 × 32 etc.) will be used in the 5G mm-wave system to avoid the above consequences. As we go for the BM design of 16 × 16 or 32 × 32 without crossover, the structure will become more complicated and difficult to route to a large number of antennas. At the same time, the performance parameter will also degrade. So, it is concluded that BM without a crossover is only applicable for a small network of 5G PAA system with high frequency but not advisable for the 5G PAA system that needs a large BM network.

4) BM WITHOUT/MODIFIED PHASE-SHIFTER

A novel compact BM without phase-shifter was presented in [69]. Fig. 6 shows that the proposed BM consisted of BLC that has −45° and −90° phase difference and a crossover. The phase-shifter was not needed in this BM because −45°

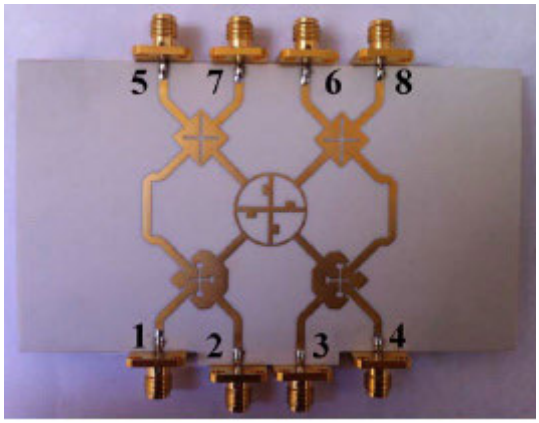

FIGURE 6. Layout of 4 × 4 BM without Phase-shifter [69].

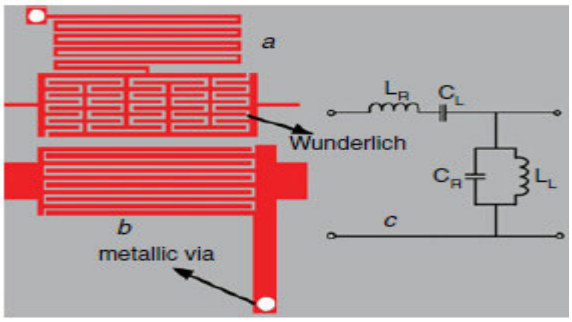

FIGURE 7. Layout of metamaterial unit-cell based on Wunderlich-shaped dentiform and meandered-line short-circuited stub to design BM [74].

phase difference was induced by using the BLC based on a chamfer patch with dumb-bell slots, and a square patch with crossed slots was used to develop −90° phase difference in the BLC. The design and fabrication of a compact BM using mitered bends were provided in [70]. The size was compact, and the TLs were spaced as close to each other as possible. In [71], a 4 × 4 BM operating at 2GHz was designed without phase-shifter, and a crossover had been presented. The phase-shifter was replaced by modifying the conventional 90° coupler to an arbitrary phase difference coupler. The proposed BM had an advantage of reducing the area, and less power dissipation was achieved by removing the phase-shifter and crossover. Researchers in [72] presented a wide-band 4 × 4 BM, which was realized by cascading the phase-shifter, crossover, and coupler.

Table 4 shows the summary of BM with and without the modified phase-shifter technique. In [69] and [71], the overall size of the BM was reduced without phase-shifters, but this seriously affected the insertion-loss for the design presented in [69]. Whereas, BM design in [71] achieved good insertion-loss in simulation, but no measured result was presented. In research articles [70] and [72], the design was based on modifying the phase-shifter. The design in [70] has a narrow bandwidth and [72] has a wide-band with large size of BM due to cascading of the components. Finally, it is concluded that the BM with or without a modified phase-shifter is not applicable for 5G BFNs because most of the design either affect the bandwidth, performance parameters, or the size.

5) BM WITH MTM-TLS

In [73], symmetric double spiral-lines (SDSLs) structure was used to develop the novel electromagnetic (EM) MTM-TL (EM-MTM-TL). The proposed BM using EM-MTM-TL was operated at 0.86GHz. Xu *et al.* [74] presented a compact BM design based on Wunderlich-shaped dentiform, as shown in Fig. 7. The meandered-line short-circuited stub inductor was used in this design to develop a composite right/left-handed TL (CRLH-TL) structure that operated at 1.8GHz. In [75], the PAA system based on BM based BFN used a 3 × 1 circular electromagnetic bandgap (EBG), which had been placed between the antenna elements to improve the gain and radiation performance at 14.5GHz. The article [76] proposed a lumped-element solution to miniaturize the BFNs. The lumped element unit-cell was used as a new class of MTM structure (tensor-TL-MTM). A miniaturized quadrature hybrid coupler, a rat-race coupler, and a 4 × 4 BM based on microstrip quasi-lumped elements that developed MTM-TL were presented in [77]. In [78], a compact 4 × 4 BM with optical transparency (OT) operating at 2.4GHz for Wi-Fi applications was proposed. The ground plane of each transparent TL in the BM was patterned with a complementary square split-ring resonator (CS-SRRs). In [79], [80], a MTM based 4 × 4 compact BM operating at 3.5GHz was presented. The MTM-TL was achieved by using an inter-digital capacitor and open coupled-lines that reduced the size by 75%, and bandwidth improved by 16%. An artificial magnetic conductor based on 'bed of nails' was used to develop 4 × 4 BM, as reported in [81]. The proposed BM operated in the frequency range of 27-29GHz with a return-loss of less than −15dB. The structure was more compact and provided improved bandwidth as well as better performance parameters.

Table 5 shows a summary of the BM with the MTM-TL technique. The analysis was done at different operating frequencies, bandwidth, performance parameters, and size reduction. From the summary, it was understood that the insertion-loss was always in the range of -7 ± 1dB, and the average phase-error of ±4° for the frequency range of 0.8GHz to 28GHz as presented in [73]–[81]. This led to the understanding that the insertion-loss did not increase with respect to the change in the operating frequency. Excellent size reduction and bandwidth improvement were achieved using this technique. The structure was not very complex as we increased the BM network size to 8 × 8 or 16 × 16 etc., because the MTM technique was applied without changing the conventional BM structure. From this, it can be concluded that the BM using MTM-TL is an ideal option for 5G BFN.

B. TRI-LAYER STRUCTURE DESIGN

The benefits of having more than one layer were taken from different papers and are summarized in this section.

TABLE 4. Review on BM without / modified phase-shifter.

Ref. / Year	ε_r , h	f_o (GHz)	Technology	Insertion-loss / Phase-error	Bandwidth Improvement / Size reduction	Return-loss / Isolation-loss
[69] / 2014	3.55, 0.813mm	6	BM consists of BLC that has -45° and -90° phase difference and a crossover	-6 to -9dB / ± 0.90°	20.1% / 40%	< -15dB / < -15dB
[70] / 2005	4.4, 1.6mm	2.4	Compact BM using mitered bends	-10.7dB / 2.4°	8.3% / -	-26dB / -35dB
[71] / 2019	-	2	BM without phase-shifter	-6 ± 0.5dB / ±1°	-	-29dB / -29dB
[72] / 2007	2.2, 0.254mm	10	BM with modified phase-shifter using coupled lines	-6.7 ± 0.7dB / 10°	20.1% / -	-40dB / -40dB

TABLE 5. Review on BM with MTM-TLs.

Ref. / Year	ε_r , h	f_o (GHz)	Technology	Insertion-loss / Phase-error	Bandwidth Improvement / Size reduction	Return-loss / Isolation-loss
[73] / 2014	2.2, 0.508mm	0.8	Symmetric double spiral lines (SDSLs)	-6.7 ± 0.5dB / ±3.1°	20% / 80.9%	-25dB / -29dB
[74] / 2011	-	1.8	Wunderlich-shaped dentiform and meandered-line short-circuited stub inductor	-7 ± 0.5dB / ±4°	12% / 45%	-25.6dB / -20dB
[75] / 2015	4.4, 1.6mm	14.5	3×1 planar circular Electromagnetic band-gap (EBG)	-7 ± 0.7dB / ±6°	-	-38dB / -28dB
[76] / 2013	2.2, 0.508mm	1	Miniaturization of BFN achieved by lumped element unit-cell	-7 ± 0.5dB / ±7°	8% / 25%	-25dB / -20dB
[77] / 2007	3.38, 0.508mm	0.915	Microstrip quasi-lumped elements incorporated to TL	-7.5 ± 1dB / ±3.46°	17% / 79%	-32.7dB / -20dB
[78] / 2016	3, 1.6mm	2.4	Complementary square SRR used in ground plane	-6.8 ± 0.5dB / ±4°	10% / 16.6%	-16dB / -20dB
[80] / 2020	4.3, 1.66mm	3.5	BM using interdigital capacitor and open coupled lines	-7 ± 1dB / ± 5°	16% / 75%	-15dB / -15dB
[81] / 2020	3.55, 0.508mm	28	Artificial magnetic conductor technology	-7 ± 1dB / ± 5°	-	-30dB / -30dB

Such layers were used to solve the crossover problem, where one line passes over a layer while the other passes through the second layer. New designs were found for the coupler, where the coupler was split into two sections, each on a separate layer. The two parts communicate with each other via a coupling mechanism. The same goes for phase-shifter. A new method has also been introduced, the technique of flipping between the two layers. This method can be accomplished by the use of via holes. However, it works mainly with the lower frequency bands. Some other techniques are needed for the higher frequencies.

These three layers of metal can be classified into two categories based on the location of the ground layer, as seen in Fig. 8(a-b). The researchers in papers [82]–[89] put the ground layer in the center of the two metallic layers, as seen in Fig. 8(a). On the other side, some other researchers in papers [90]–[93] have put the ground layer on the bottom, as shown in Fig. 8(b), respectively.

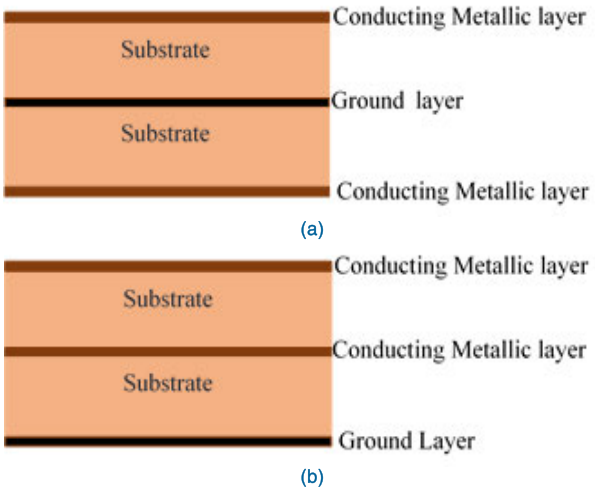

FIGURE 8. (a) Metal-Ground-Metal BM Structure (b) Metal-Metal-Ground BM Structure.

In [82], the BM was constructed using multi-layer technology. Two different designs of the coupler were presented in the paper to construct the BM. The first design was based on two lozenge-shaped conductors placed on the bottom and top layers, and a hexagonal slot etched in the common ground plane was used to couple between the two layers. In the second design, two elliptical-shaped conductors, and an elliptical slot were used.

A low-cost 8 × 8 BM was introduced in [83], which operated at 4.3 GHz based on a novel multi-layer microstrip design. Three directional BLCs were used as the 3dB / 90° bridge, and a type of enhanced Schiffman phase-shifter was used as a fixed phase-shifter. This technique reduced the size and enhanced the operational bandwidth of the proposed design.

In [84], a novel 4 × 4 BM was proposed, which consisted of four 3dB directional couplers and two 45° phase-shifters placed on the bi-layer substrate. The proposed BM was implemented using a dual conducting layer between the double-layer substrate that consisted of two 45° phase-shifters and four 3-dB directional couplers. In this design, Port-1 and Port-3 were connected to the upper, whereas Port-2 and Port-4 were connected to the lower conductor layer, respectively. In the common ground layer, there was an ellipse slot that allowed the coupling between the two layers.

A novel ultra-wideband (UWB) 4 × 4 BM that operated between 3.1GHz-10.6GHz was presented in [85]. The novel idea proposed in this work was the butterfly-shaped design for layer interconnection, which was also used in the coupler. The hybrid coupler of the proposed BM was constructed using two TLs on separate layers, whereas the butterfly-shaped interconnection design ensured the connection between them. On one layer, the feeding and the direct ports were printed, and on the other layer, the coupled and the isolated ports were applied. There was an open hole in the common ground layer that allowed the coupling between the two layers.

In [86], a compact 4 × 4 UWB BM that operated between 3GHz-10.6GHz was presented. Fig. 9 shows that the proposed 4 × 4 BM consisted of four slot-coupled directional couplers that has a phase difference of 90° and two relative 45° phase-shifters. The configuration is similar to [82], but the conductor and slot shape in the ground plane are different. In order to generate a relative 45° phase-shift, the same design of the coupler was used.

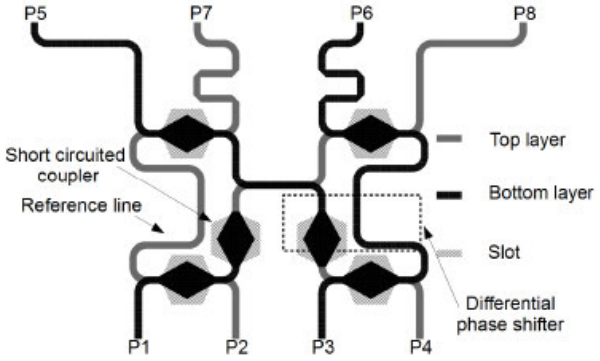

FIGURE 9. Layout of ultra wide-band 4 × 4 tri-layer BM design [86].

Using the co-planar waveguide (CPW) technology [87], a novel 4 × 4 tri-layer BM based on a two-layer slot-coupled method was presented, which operated at 5.8GHz. This BM used 3dB CPW directional slot-coupled couplers and wide-band multi-layer 3dB CPW BLC, and a phase-shifter. The rectangular slot was etched on the ground plane, which allowed the coupling between CPW lines placed in the upper and lower conducting layers.

The article [88] has proposed a tri-layered BM circuit for the feeding of multi-beam antenna systems. The feeding circuits on the upper and lower layers were connected by the slot on the common ground plane, which generates the completion of the directional and hybrid coupler. The port configuration was similar to the one presented in reference [84].

Substrate integrated waveguide (SIW) technology was proposed by researchers in [89] to design and fabricate a wide-band bi-layer 4 × 4 BM. The two-fold enhancement method was used to develop a two-layer SIW design.

Article [90] presented a novel tri-layer configuration of a 16 × 16 BM that operated at 2GHz. A high-temperature superconductor (HTS) was used for the fabrication of this proposed BM. The tri-layer configuration made the size compact by removing the microstrip-line crossovers, and slot technology was used to couple between the top layer and bottom layer, respectively.

In [91], the miniaturization of BM was achieved by a novel slow-wave structure with a high slow-wave factor, as shown in Fig. 10. The novel slow-wave structure was based on meandered-line, inter-digital TL, and low-impedance TL. The proposed 4 × 4 BM showed a size reduction of 94.2% as compared to the conventional ones.

The 4 × 4 BM which composed of six three-section couple-lines directional couplers and C-section Schiffman phase-shifter was presented in [92]. For the crossover,

TABLE 6. Review on tri-layer BM based on metal-ground-metal structure.

Ref. / Year	ε_r , h	f_o (GHz)	Technology	Insertion-loss / Phase-error	Bandwidth Improvement / Size reduction	Return-loss / Isolation-loss
[82] / 2017	3.38 0.508mm	3.1 - 10.6	Multi-layer technology using coupler and phase-shifter without using crossover	-7 ± 2dB / ± 13 °	Wide-band (7.5GHz) / -	< -13dB / < -13dB
[83] / 2014	2.55, 0.88mm	4.3	Three-directional BLCs and Schiffman phase-shifter has been proposed to avoid using crossover to design 8×8 BM	-7 ± 2.5dB / ± 15 °	23% / -	< −10dB / -17dB
[84] / 2014	4.3, 0.8mm	2.45	Dual TL on double-layer structure	-7 ± 2.5dB / ± 8°	-	< −10dB / < −10dB
[85] / 2013	2.2, 0.508mm	3.1 - 10.6	Butterfly shaped microstrip designed for layer interconnection without crossover	-7.5 ± 2.5dB / ± 10°	Wide-band (7.5GHz) / -	< −10dB / < −17dB
[87] / 2006	2.2, 0.254mm	5.8	BM based on a two-layer slot-coupled using CPW technology without using any crossovers	-7.5 ± 1dB / ±9°	5.17% / -	-25dB / -20dB
[88] / 2014	4.3, 1.6mm	2	Feeding circuit on upper and lower layers are connected by a slot on the common ground plane that generates the completion of directional and hybrid coupler	-7 ± 2dB / ±8°	-	-20dB / -15dB
[89] / 2011	2.94, 0.508mm	12.5	Tri-layer substrate integrated waveguide (SIW) technology	-7 ± 1dB / ±10°	24% / -	-12dB / -15dB

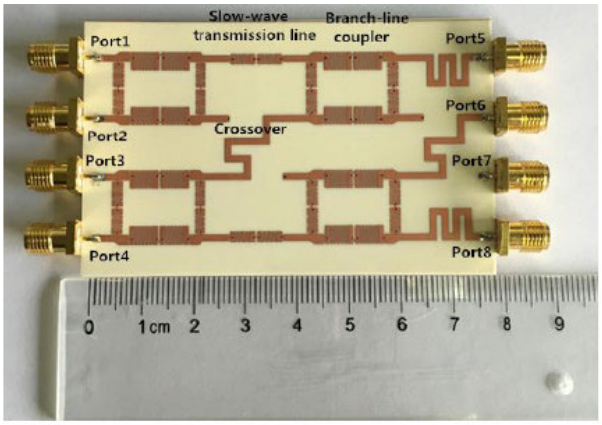

FIGURE 10. Tri-layer BM based on slow wave structure [91].

two of those couplers were used. The BM operated at the center frequency of 3GHz and achieved a bandwidth of almost 2GHz.

The article [93] introduced a novel multiport broadband measurement device that used a regular 8 × 8 BM. The proposed measuring method consisted of only one 8 × 8 broadband BM and only one isolator, enabling the measurement of all matrix coefficients of any two-port units.

Table 6 and 7 show the detailed summary of the tri-layer structure using a common ground layer and bottom ground layer, respectively. The BM using the tri-layer structure improved the bandwidth and reduced the size. As shown by the summary of the result in Table 6, the insertion-loss was very high due to the coupling between the two-layers through the common ground slot, and it drastically increased as the frequency went above 9GHz [85], [86]. Article [89] presented their work at 12.5GHz, which improved the insertion-loss but increased the phase-error. In the case of a tri-layer structure with bottom ground plane, it has a better result than a tri-layer structure with a common ground plane. The analysis also found that fabrication is a little complicated, and it is difficult for large BM networks.

C. FOUR-LAYER STRUCTURE DESIGN

A four-layer structure had accompanied quite a few papers. As illustrated in Fig. 11, it is like the "common bottom layer" structure with an extra ground layer at the top.

As shown in Fig. 12, a novel four-layer structure based 4 × 4 BM was designed and realized in [94] by using SIW technology. It has a wide-band operating frequency range of over 8.5 to 10.6 GHz with excellent performance in phase and amplitude. The Ku-band 4 × 4 BM was presented in [95].

TABLE 7. Review on tri-layer BM based on metal-metal-ground structure.

Ref. / Year	ε_r , h	f_o (GHz)	Technology	Insertion-loss / Phase-error	Bandwidth Improvement / Size reduction	Return-loss / Isolation-loss
[90] / 2003	24, 0.5mm	2	High-temperature superconductor (YBCO) was used as conducting metallic and ground plane Tri-layer 8x8 BM configuration	-7 ± 1dB / ±5°	-	-15dB / -15dB
[91] / 2017	3.38, 0.203mm	0.970	Novel structure with high slow-wave factor	-6.5 ± 1dB / ±2°	- / 94.2%	-25dB / -20dB
[92] / 2010	3.4 / 3.38 / 3.2, 0.05mm / 0.099mm / 0.787mm	3	Multi-layer BM consist of six three-section couple-line directional couplers Schiffman C-section phase-shifter	7 ± 0.9dB & ±10°	60% / -	-16dB / -21dB
[93] / 2014	-	2 - 3.5	Multiport broadband measurement device that uses a regular 8x8 BM	7 ± 1dB & ±8°	-	<-10dB / <-15dB

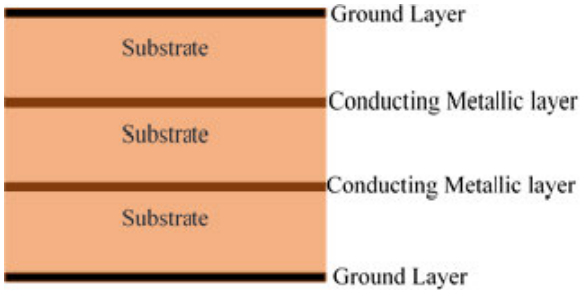

FIGURE 11. Four-layer Ground-Metal-Metal-Ground BM Structure.

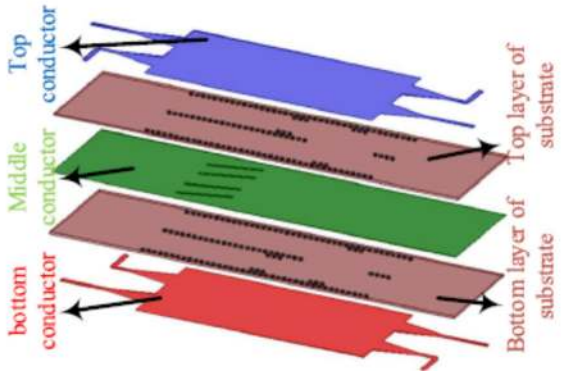

FIGURE 12. Four-layer BM based on SIW technology [94].

The proposed BM consisted of 3dB hybrid BLC and a crossover that was designed using the SIW method. It operated at the center frequency of 12.5GHz, having an excelling amplitude and phase performance over a bandwidth of 3GHz.

In [96], a 4×4 BM having broadband amplitude and phase characteristics was designed using the multi-layer microstrip technique. The multi-layer directional coupler was utilized as a basic element of the BM. It consisted of four 3dB / 90° directional couplers, two 45° phase-shifters, and a TL crossover. A SIW based four-layer 4×4 BM that operated at center frequency 60GHz was presented in [97]. The proposed BM achieved a size reduction of 60% and operated in the frequency band of 55-65GHz. Table 8 shows a detailed summary of the four-layer BM structure. From the summary, it is understood that this technique has improved BW, size reduction, and performance parameters. It is not applicable for large BM networks like 16×16, 32×32, etc. due to the fabrication complexity. It is advisable for only a smaller BM network size.

III. SUMMARY

This section will summarize the amount of research that had been done by the researchers using different layers of BM. It is important to note that much of the research work was performed using the bi-layer BM system, whereas the complex geometries like tri-layer and four-layer BM were avoided due to difficult fabrication issues

Table 9 summarizes the performance parameters, bandwidth, compact size, and fabrication complexity of BM using bi-layer, tri-layer, and four-layer, respectively. Table 9 shows whether different BM designs satisfy certain acceptance criteria or not. Most of the techniques achieved better insertion-loss at a lower frequency, but for the higher frequencies, the techniques like BM without crossover, BM with MTM-TL, and four-layer BM are the only techniques that satisfy the insertion-loss criteria. Large BM networks like 8×8, 16×16, etc., do not achieve better insertion-loss except BM with MTM-TL. Moreover, the power division to the antennas will also be difficult due to the complexity in

TABLE 8. Review on four-layer BM based on ground-metal-metal-ground structure.

Ref. / Year	ε_r , h	f_o (GHz)	Technology	Insertion-loss / Phase-error	Bandwidth Improvement / Size reduction	Return-loss / Isolation-loss
[94] / 2015	3.55, 0.508mm	8.5 - 10.6	SIW without crossover	-6 ± 1dB / ±5°	22% / 35%	<-15dB / <-20dB
[95] / 2010	2.33, 0.787mm	12.5	SIW hybrid 3-dB coupler and crossover	-7.5 ± 1dB / 12.5°	24% / -	<-15dB / <-20dB
[96] / 2007	2.33 / 2.28 / 3.2, 0.127mm / 0.038mm / 0.787mm	2.2	Multi-layer directional coupler is utilized as a basic element of BM	-7 ± 0.8dB / ±7°	-	<-25dB / <-25dB
[97] / 2011	5.7, 0.094	60	SIW	-7 ± 1dB / ±4°	16.6% / 60%	-35dB /-25dB

TABLE 9. Summary of all BM techniques discussed in this paper.

Technique	Insertion-loss (-7dB) at lower frequency	Insertion-loss (-7dB) at higher frequency	Insertion-loss for large size BM network	Phase-error below ±7°	Bandwidth	Compact size	Return-loss and Isolation-loss below -15dB	Fabrication Complexity	Cost
BM with open-stub	x	x	x	x	√	√	√	Simple	Low
BM with modified BLC	√	x	x	√	√	√	√	Simple	Low
BM without crossover	√	√	x	√	√	√	√	Simple	Low
BM without Phase-shifter	x	x	x	√	x	√	√	Simple	Low
BM with MTM-TL	√	√	√	√	√	√	√	Simple	Low
Tri-layer BM	x	x	x	x	√	√	√	Complex	High
Four-layer BM	√	√	x	√	√	√	√	Complex	High

the shape of a large BM structure. In this research study, most of the discussed techniques modify the configuration of the conventional BM structure to achieve size reduction. Although, when the MTM-TL technique is applied to the BM components, they do not change the configuration of the conventional BM structure. So, it will be challenging for the BM technique other than MTM-TL to construct a large BM network with good performance parameters and routing the power to the antenna.

Fig. 13 shows a bar graph of bi-layer BMs described in this article, which demonstrates the size reduction and bandwidth. From the bar graph, it can be seen that research articles [42], [44], [54], [73], [77], [80] have shown a size reduction of above 70%, and also articles [53], [58], [61], [62], [73] have bandwidth improvement of above 25% as compared to the conventional BM. Some of the researchers in their papers, for example [60]–[64], [68] have only reported the bandwidth improvement results, and no discussion on the size reduction was provided, as shown in the bar graph in Fig. 13.

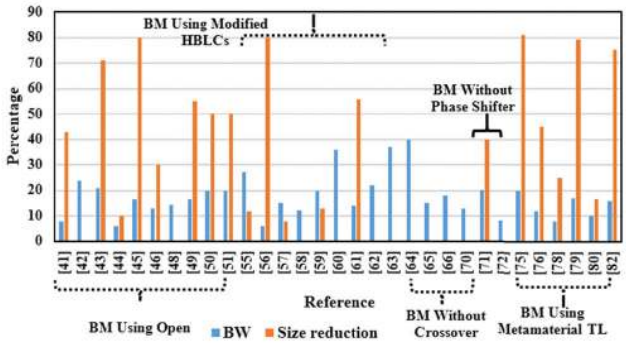

FIGURE 13. Bar graph of bi-layer BM research papers that show the bandwidth (BW) improvement and size reduction with respect to conventional BM design [27].

The other most interesting fact that is identified from the results presented in the bar graph is that the MTM based bi-layer BM system achieved a size reduction of 80% and a bandwidth improvement of 20%. Tri-layer and four-layer

BM technique achieved excellent bandwidth improvement, but the performance parameters like phase-error, insertion-loss, isolation-loss, and return-loss were not up to the mark as compared to the bi-layer BM technique. The fabrication process of the tri-layer and four-layer is cumbersome and expensive. So, most of the work has been carried out using a bi-layer structure due to easy fabrication, enhanced bandwidth, and compact size.

In the review, most of the research work was performed in the frequency range between 1-3GHz. Few researchers have worked above 3GHz, i.e., in the 5G wireless communication frequency bands and large BM network due to complex design geometries and strict fabrication tolerances. As discussed in the literature [98]–[101], the upcoming 5G and next-generation B5G are considered modern wireless technologies, so while designing BFNs for the PAA systems, researchers can use the finding presented in this paper and make better decisions as to which BM design will be more suitable as per their requirements.

IV. CONCLUSION / FUTURE WORK

This paper has presented an exhaustive review of the Butler Matrix (BM) based Beamforming Networks (BFNs), which are considered an integral part of the phased array antennas (PAAs) in the upcoming 5G systems. The main aim of this paper is to provide a comprehensive literature survey and comparison of the results presented by several researchers on various types of BM based on bi-layer, tri-layer, and four-layer design techniques.

Through the analysis of the literature, it is found that the first BM was introduced by Butler and Lowe [27], and it had limitations of narrow bandwidth and is large in size. Since then, many unique and novel structures have been developed and presented by researchers to solve conventional BM design limitations. This is discussed in detail in the bi-layer BM structure section of this paper. From the data presented in Tables and summarized in the bar graph, it is found that some BM designs presented by researchers increased the bandwidth while others reduced the size, and some paper worked on both limitations marginally. Moreover, the problem of the crossover was solved by some researchers by using four-layer based BM. However, it is understood from the results summarized in Section II (B) and II (C), respectively, that the performance parameters like phase-error/insertion-loss are more at lower frequencies for tri-layer as compared to bi-layer BM. So, they are not recommended for high frequency operations. The four-layer BM achieved better insertion-loss / phase-error at lower and higher frequency, but due to the complexity of fabrication for a large BM network, it is not advisable for 5G BFN.

It is a known fact that the BFNs, such as BM plays a crucial role in 5G [98], [99] and B5G [100], [101] antenna array systems to achieve wide coverage and high-gain. The main requirement of BFNs for 5G and B5G technology is to have low insertion and power loss, high bandwidth, compact size, low fabrication cost, and conformity to the system. It is understood from the detailed literature review presented in this paper that bi-layer BM is a simple geometry compared to other BM techniques, and it also solved the problem of crossover, large size, and narrow bandwidth. Based on the data summarized in Table 5 and 9, and the bar graph presented in Fig. 13, it is recommended by the author to use metamaterial (MTM) based bi-layer BM for the 5G and B5G PAA system BFNs. This is due to their low insertion-loss and phase-error at any frequency/large BM network, compact size, excellent bandwidth, good S-parameter performance, and low in profile nature and fabrication cost. Quite recently, the International Wireless Industry Consortium (IWPC) [102] published a white paper on 5G mm-wave frequencies and mobile networks, which suggests that MTM structures have become one of the most common techniques to address the problems of the 5G mm-wave PAA systems in the recent years. Another problem at the mm-wave frequency bands is that different components of the BM will have very thin microstrip-lines, which leads to a complex fabrication process. So, to overcome this issue, the use of BM with MTM structure is recommended [81]. In the future, it will be important to consider advanced/novel MTMs, and precision fabrication techniques for the development of BFNs for 5G and B5G antenna array systems.

REFERENCES

[1] S. P. Guerouni, "Multibeam antenna terminal for wireless local area network," in *Proc. IEEE-APS Conf. Antennas Propag. Wireless Commun.*, Nov. 2000, pp. 141–142.

[2] T. Cao Quyen and T. Anh Vu, "The application of a multibeam antenna for 4G," in *Proc. Int. Conf. Adv. Technol. Commun.*, Oct. 2012, pp. 227–230.

[3] W. Hong, Z. H. Jiang, C. Yu, J. Zhou, P. Chen, Z. Yu, H. Zhang, B. Yang, X. Pang, M. Jiang, Y. Cheng, M. K. T. Al-Nuaimi, Y. Zhang, J. Chen, and S. He, "Multibeam antenna technologies for 5G wireless communications," *IEEE Trans. Antennas Propag.*, vol. 65, no. 12, pp. 6231–6249, Dec. 2017, doi: 10.1109/TAP.2017.2712819.

[4] W. Hong, P. Chen, Y. Cheng, J. Zhou, Z. Kuai, and K. Wu, "Multibeam antennas for next generation mobile communications and mobile satellite communications," in *Proc. Loughborough Antennas Propag. Conf.*, Mar. 2008, pp. 58–61.

[5] O. Lafond and M. Himdi, "Multibeam antenna in millimeter waves," in *Proc. 32nd Eur. Microw. Conf.*, Oct. 2002, pp. 1–4.

[6] B. Schoenlinner and G. M. Rebeiz, "Compact multibeam imaging antenna for automotive radars," in *IEEE MTT-S Int. Microw. Symp. Dig.*, vol. 2, Jun. 2002, pp. 1373–1376.

[7] J. B. L. Rao, R. Mital, D. P. Patel, M. G. Parent, and G. Tavik, "Low-cost multibeam phased array antenna for communications with GEO satellites," *IEEE Aerosp. Electron. Syst. Mag.*, vol. 28, no. 6, pp. 32–37, Jun. 2013.

[8] Q.-L. Yang, Y.-L. Ban, K. Kang, C.-Y.-D. Sim, and G. Wu, "SIW multibeam array for 5G mobile devices," *IEEE Access*, vol. 4, pp. 2788–2796, 2016.

[9] M. Uthansakul and P. Uthansakul, "Experiments with a low-profile beamforming MIMO system for WLAN applications," *IEEE Antennas Propag. Mag.*, vol. 53, no. 6, pp. 56–69, Dec. 2011.

[10] Y. M. Cheng, P. Chen, W. Hong, T. Djerafi, and K. Wu, "Substrate-Integrated-Waveguide beamforming networks and multibeam antenna arrays for low-cost satellite and mobile systems," *IEEE Antennas Propag. Mag.*, vol. 53, no. 6, pp. 18–30, Dec. 2011.

[11] A. K. Pandey, "Design of a compact high power phased array for 5G FD-MIMO system at 29 GHz," in *Proc. Asia–Pacific Microw. Conf. (APMC)*, Dec. 2016, pp. 1–4.

[12] J.-H. Kim, J.-H. Han, J.-S. Park, and J.-G. Kim, "Design of phased array antenna for 5G mm-wave beamforming system," in *Proc. IEEE 5th Asia–Pacific Conf. Antennas Propag. (APCAP)*, Jul. 2016, pp. 201–202.

[13] T. A. Denidni and T. E. Libar, "Wide band four-port butler matrix for switched multibeam antenna arrays," in *Proc. 14th IEEE Proc. Pers., Indoor Mobile Radio Commun.*, vol. 3, Sep. 2003, pp. 2461–2464.

[14] C. Collado, A. Grau, and F. De Flaviis, "Dual-band butler matrix for WLAN systems," in *IEEE MTT-S Int. Microw. Symp. Dig.*, Dec. 2005, p. 4.

[15] P. Angeletti and M. Lisi, "Multimode beamforming networks for space applications," *IEEE Antennas Propag. Mag.*, vol. 56, no. 1, pp. 62–78, Feb. 2014.

[16] G. Rosati and J. Munn, "Fast prototyping of an 8×8 butler matrix beamforming network for 5G applications," in *Proc. Int. Conf. Electromagn. Adv. Appl. (ICEAA)*, 2017, pp. 1029–1032.

[17] P. S. Hall and S. J. Vetterlein, "Review of radio frequency beamforming techniques for scanned and multiple beam antennas," *IEE Proc. H-Microw., Antennas Propag.*, vol. 137, pp. 293–303, Oct. 1990.

[18] S. Vashist, M. K. Soni, and P. K. Singhal, "A review on the development of rotman lens antenna," *Chin. J. Eng.*, vol. 14, no. 11, pp. 1–9, 2014. Accessed: Oct. 18, 2017. [Online]. Available: https://www.hindawi.com/journals/cje/2014/385385/

[19] R. Walter, "Multiple beam radar antenna system," U.S. Patent 3 170 158 A, Feb. 16, 1965.

[20] M. A. Hassanien, M. Jenning, and D. Plettemeier, "Beam steering system using rotman lens for 5G applications at 28 GHz," in *Proc. IEEE Int. Symp. Antennas Propag. USNC/URSI Nat. Radio Sci. Meeting*, Jul. 2017, pp. 2091–2092.

[21] M. Rajabalian and B. Zakeri, "Optimisation and implementation for a non-focal rotman lens design," *IET Microw., Antennas Propag.*, vol. 9, no. 9, pp. 982–987, Jun. 2015.

[22] A. A. Jneibi, M. A. Marri, E. A. Hadhrami, M. A. Mufti, S. Triantafyllidis, A. Konstantinidis, M. S. Khan, and R. Shubair, "Design of a wideband phased array transmitter using rotman lens," in *Proc. IEEE Asia–Pacific Microw. Conf. (APMC)*, Nov. 2017, pp. 256–259.

[23] A. Pautz, M. Hagelen, and R. Kulke, "Multiple target detection using rotman lens beamforming," in *Proc. 18th Int. Radar Symp. (IRS)*, Jun. 2017, pp. 1–10.

[24] P. Simon, "Analysis and synthesis of Rotman lenses," in *Proc. 22nd AIAA Int. Commun. Satell. Syst. Conf. Exhibit (ICSSC)*, Monterey, CA, USA, May 2004, p. 3196, doi: 10.2514/6.2004-3196.

[25] J. Blass, "Multidirectional antenna–A new approach to stacked beams," in *Proc. IRE Int. Conv. Rec.*, 1960, vol. 8, pp. 48–50.

[26] J. Nolen, "Synthesis of multiple beam networks for arbitrary illuminations," Ph.D. dissertation, Radio Division, Bendix Corp., Baltimore, MD, USA, Apr. 1965.

[27] J. Butler and R. Lowe, "Beam-forming matrix simplifies design of electronically scanned antennas," *Electron. Des.*, vol. 9, pp. 170–173, Apr. 1961.

[28] I. Sfar, L. Osman, and A. Gharsallah, "Design of a 4×4 butler matrix for beamforming antenna applications," in *Proc. Medit. Microw. Symp.*, vol. 2014, pp. 1–4.

[29] *Study on Implications of 5G Deployment on Future Business Models*. Accessed: Oct. 8, 2018. [Online]. Available: https://berec.europa.eu/eng/document_register/subject_matter/berec/reports/8008-study-on-implications-of-5g-deployment-on-future-business-models

[30] P. Pirinen, H. Pennanen, A. Pouttu, T. Tuovinen, N. Tervo, P. Luoto, and M. Latva-aho, , "RF driven 5G system design for centimeter waves," *Wireless Commun. Mobile Comput.*, vol. 2018, Jan. 2018, Art. no. 7852896.

[31] W. Hong, K.-H. Baek, Y. Lee, Y. Kim, and S.-T. Ko, "Study and prototyping of practically large-scale mmWave antenna systems for 5G cellular devices," *IEEE Commun. Mag.*, vol. 52, no. 9, pp. 63–69, Sep. 2014, doi: 10.1109/MCOM.2014.6894454.

[32] N. Ojaroudi Parchin, M. Alibakhshikenari, H. Jahanbakhsh Basherlou, R. A. Abd-Alhameed, J. Rodriguez, and E. Limiti, "MM-wave phased array quasi-yagi antenna for the upcoming 5G cellular communications," *Appl. Sci.*, vol. 9, no. 5, p. 978, Mar. 2019, doi: 10.3390/app9050978.

[33] T. S. Rappaport, S. Sun, R. Mayzus, H. Zhao, Y. Azar, K. Wang, G. N. Wong, J. K. Schulz, M. Samimi, and F. Gutierrez, "Millimeter wave mobile communications for 5G cellular: It will work!," *IEEE Access*, vol. 1, pp. 335–349, 2013, doi: 10.1109/ACCESS.2013.2260813.

[34] R. Mendez-Rial, C. Rusu, N. Gonzalez-Prelcic, A. Alkhateeb, and R. W. Heath, Jr., "Hybrid MIMO architectures for millimeter wave communications: Phase shifters or switches?" *IEEE Access*, vol. 4, pp. 247–267, 2016, doi: 10.1109/ACCESS.2015.2514261.

[35] T.-Y. Chin, S.-F. Chang, J.-C. Wu, and C.-C. Chang, "A 25-GHz compact low-power phased-array receiver with continuous beam steering in CMOS technology," *IEEE J. Solid-State Circuits*, vol. 45, no. 11, pp. 2273–2282, Nov. 2010, doi: 10.1109/JSSC.2010.2064010.

[36] M. Rihan, T. Abed Soliman, C. Xu, L. Huang, and M. I. Dessouky, "Taxonomy and performance evaluation of hybrid beamforming for 5G and beyond systems," *IEEE Access*, vol. 8, pp. 74605–74626, 2020, doi: 10.1109/ACCESS.2020.2984548.

[37] A. Naqvi and S. Lim, "Review of recent phased arrays for millimeter-wave wireless communication," *Sensors*, vol. 18, no. 10, p. 3194, Sep. 2018.

[38] A. T. Alreshaid, M. S. Sharawi, S. Podilchak, and K. Sarabandi, "Compact millimeter-wave switched-beam antenna arrays for short range communications," *Microw. Opt. Technol. Lett.*, vol. 58, no. 8, pp. 1917–1921, Aug. 2016.

[39] P. Yazdanbakhsh and K. Solbach, "Microstrip Butler matrix design and realization for 7 T MRI," *Magn. Reson. Med.*, vol. 66, no. 1, pp. 270–280, Jul. 2011.

[40] P. Bhowmik and T. Moyra, "Modelling and validation of a compact planar butler matrix by removing crossover," *Wireless Pers. Commun.*, vol. 95, no. 4, pp. 5121–5132, Aug. 2017.

[41] S. Zheng, W. S. Chan, S. H. Leung, and Q. Xue, "Broadband butler matrix with flat coupling," *Electron. Lett.*, vol. 43, no. 10, pp. 576–577, May 2007.

[42] S. Zheng and W. S. Chan, "Compact butler matrix using size reduced elements," *Microw. Opt. Technol. Lett.*, vol. 49, no. 7, pp. 1519–1521, Jul. 2007.

[43] H. Hayashi, D. A. Hitko, and C. G. Sodini, "Four-element planar butler matrix using half-wavelength open stubs," *IEEE Microw. Wireless Compon. Lett.*, vol. 12, no. 3, pp. 73–75, Mar. 2002.

[44] T. K. G. Kwang and P. Gardner, "4×4 butler matrix beam forming network using novel reduced size branchline coupler," in *Proc. 31st Eur. Microw. Conf.*, Sep. 2001, pp. 1–4.

[45] S. K. A. Rahim and P. Gardner, "Beamforming networks using cascaded butler matrices," in *Proc. Asia–Pacific Conf. Appl. Electromagn.*, Dec. 2007, pp. 1–4.

[46] S. Kuwana, H. Hayashi, and R. Ueda, "Simple design of four-element planar butler matrix using two-section branch-line hybrids," *IEEJ Trans. Electr. Electron. Eng.*, vol. 12, pp. S187–S188, Jun. 2017.

[47] W. Nie, Y. Fan, S. Luo, and Y. Guo, "A switched-beam microstrip antenna array with miniaturized butler matrix network," *Microw. Opt. Technol. Lett.*, vol. 57, no. 4, pp. 841–845, Apr. 2015.

[48] C. Chen, H. Wu, and W. Wu, "Design and implementation of a compact planar 4×4 microstrip butler matrix for wideband application," *Prog. Electromagn. Res. C*, vol. 24, p. 13, 2011.

[49] K. Klionovski, M. S. Sharawi, and A. Shamim, "A dual-polarization-switched beam patch antenna array for millimeter-wave applications," *IEEE Trans. Antennas Propag.*, vol. 67, no. 5, pp. 3510–3515, May 2019, doi: 10.1109/TAP.2019.2900438.

[50] I. I. Idrus, T. Abdul Latef, N. K. Aridas, M. S. Abu Talip, Y. Yamada, T. Abd Rahman, I. Adam, and M. N. Mohd Yasin, "A low-loss and compact single-layer butler matrix for a 5G base station antenna," *PLoS ONE*, vol. 14, no. 12, Dec. 2019, Art. no. e0226499, doi: 10.1371/journal.pone.0226499.

[51] L. Jiahui, H. Fei, Z. Runyun, C. Wenhua, T. Zhigang, and Z. Shidong, "Mmwave mobile communication under hypercellular architecture," *J. Commun. Inf. Netw.*, vol. 1, no. 2, pp. 62–76, Aug. 2016, doi: 10.11959/j.issn.2096-1081.2016.023.

[52] (Feb. 20, 2014). *Attenuation (Insertion Loss) Measurement and Testing—DTX CableAnalyzer*. Accessed: Sep. 22, 2020. [Online]. Available: https://www.flukenetworks.com/knowledgebase/dtxcableanalyzer/attenuation-insertion-loss-measurement-and-testing-dtx

[53] H. Nachouane, A. Najid, A. Tribak, and F. Riouch, "Broadband 4×4 butler matrix using wideband 90 hybrid couplers and crossovers for beamforming networks," in *Proc. Int. Conf. Multimedia Comput. Syst. (ICMCS)*, Marrakech, Morocco, Apr. 2014, pp. 14–16.

[54] M. Traii, M. Nedil, A. Gharsallah, and T. A. Denidni, "A new design of compact 4 × 4 butler matrix for ISM applications," *Int. J. Microw. Sci. Technol.*, vol. 2008, Feb. 2009, Art. no. 784526, doi: 10.1155/2008/784526.

[55] H. Ren, B. Arigong, M. Zhou, J. Ding, and H. Zhang, "A novel design of 4 × 4 butler matrix with relatively flexible phase differences," *IEEE Antennas Wireless Propag. Lett.*, vol. 15, pp. 1277–1280, 2016.

[56] D.-J. Ma, H.-L. Peng, W.-Y. Yin, and J.-F. Mao, "The realization of high isolation and wide band 4 × 4 microstrip butler matrix," in *Proc. Int. Conf. Microw. Technol. Comput. Electromagn. (ICMTCE)*, 2009, pp. 88–91.
[57] Q. P. Chen, S. L. Lai, and S. Y. Zheng, "Compact butler matrix based on patch element for x band applications," in *Proc. Asia–Pacific Microw. Conf. (APMC)*, Dec. 2015, pp. 1–3.
[58] X. Jing, S. Sun, Q. S. Liu, and Y. Li, "Study of wideband patch-based butler matrix and its high-frequency application," in *Proc. IEEE Antennas Propag. Soc. Int. Symp. (APSURSI)*, Jul. 2014, pp. 470–471.
[59] Y.-L. Li, Q. S. Liu, S. Sun, and S. S. Gao, "A miniaturised butler matrix based on patch hybrid couplers with cross slots," in *Proc. IEEE Antennas Propag. Soc. Int. Symp. (APSURSI)*, Jul. 2013, pp. 2145–2146.
[60] Y. K. Ningsih, M. Asvial, and E. T. Rahardjo, "Design and analysis of wideband nonuniform branch line coupler and its application in a wideband butler matrix," *Int. J. Antennas Propag.*, vol. 2012, pp. 1–7, 2012. Accessed: Sep. 22, 2020. [Online]. Available: https://www.hindawi.com/journals/ijap/2012/853651/
[61] S. A. Babale, S. K. Abdul Rahim, O. A. Barro, M. Himdi, and M. Khalily, "Single layered 4 × 4 butler matrix without phase-shifters and crossovers," *IEEE Access*, vol. 6, pp. 77289–77298, 2018, doi: 10.1109/ACCESS.2018.2881605.
[62] H. T. Nguyen, K. S. Ang, and G. I. Ng, "Design of a broad-band novel Butler matrix," in *Proc. Asia–Pacific Microw. Conf.*, vol. 2011, pp. 753–756.
[63] C. Dall'Omo, T. Monediere, B. Jecko, F. Lamour, I. Wolk, and M. Elkael, "Design and realization of a 4×4 microstrip butler matrix without any crossing in millimeter waves," *Microw. Opt. Technol. Lett.*, vol. 38, no. 6, pp. 462–465, Jul. 2003.
[64] X. Jing, L. J. Jiang, S. Sun, and L. Zhu, "A patch-resonator-based butler matrix with new triangular phase shifters," in *Proc. IEEE Int. Symp. Antennas Propag. (APSURSI)*, Jun. 2016, pp. 61–62.
[65] M. SalarRahimi and G. A. E. Vandenbosch, "Beam steerable subarray with small footprint for use as building block in wall-mounted indoor wireless infrastructure," *IET Microw., Antennas Propag.*, vol. 13, no. 4, pp. 526–531, Mar. 2019, doi: 10.1049/iet-map.2018.6189.
[66] Z. Mousavi and P. Rezaei, "Millimetre-wave beam-steering array antenna by emphasising on improvement of butler matrix features," *IET Microw., Antennas Propag.*, vol. 13, no. 9, pp. 1287–1292, Jul. 2019, doi: 10.1049/iet-map.2018.5340.
[67] H. Ren, J. Shao, R. Zhou, B. Arigong, and H. Zhang, "Compact phased array antenna system based on dual-band operations," *Microw. Opt. Technol. Lett.*, vol. 56, no. 6, pp. 1391–1396, Jun. 2014, doi: 10.1002/mop.28343.
[68] G. A. Adamidis, I. O. Vardiambasis, M. P. Ioannidou, and T. N. Kapetanakis, "Design and implementation of single-layer 4×4 and 8×8 butler matrices for multibeam antenna arrays," *Int. J. Antennas Propag.*, vol. 2019, pp. 1–12, Mar. 2019. Accessed: Jan. 3, 2020. [Online]. Available: https://www.hindawi.com/journals/ijap/2019/1645281/
[69] G. Tian, J.-P. Yang, and W. Wu, "A novel compact butler matrix without phase shifter," *IEEE Microw. Wireless Compon. Lett.*, vol. 24, no. 5, pp. 306–308, May 2014.
[70] P. Q. Mariadoss, M. K. A. Rahim, and M. Z. A. A. Aziz, "Design and implementation of a compact butler matrix using mitered bends," in *Proc. Asia–Pacific Microw. Conf. Proc.*, vol. 2005, vol. 5, p. 4.
[71] K. Han, W. Li, and Y. Liu, "Flexible phase difference of 4×4 butler matrix without phase-shifters and crossovers," *Int. J. Antennas Propag.*, vol. 4, p. 4, Dec. 2019. Accessed: Sep. 22, 2020. [Online]. Available: https://www.hindawi.com/journals/ijap/2019/4703161/
[72] J. He, B.-Z. Wang, Q.-Q. He, Y.-X. Xing, and Z.-L. Yin, "Wideband X-band microstrip butler matrix," *Prog. Electromagn. Res.*, vol. 74, pp. 131–140, Dec. 2007, doi: 10.2528/PIER07042302.
[73] M. Du and H. Peng, "Ultra-compact electromagnetic metamaterial transmission line and its application in miniaturized butler matrix," *Prog. Electromagn. Res. C*, vol. 55, pp. 187–197, 2014.
[74] H. X. Xu, G. M. Wang, and X. Wang, "Compact Butler matrix using composite right/left handed transmission line," *Electron. Lett.*, vol. 47, no. 19, pp. 1081–1083, Sep. 2011.
[75] W. Bhowmik, V. R. Gupta, S. Srivastava, and L. Prasad, "Gain enhancement of butler matrix fed antenna array system by using planar circular EBG units," in *Proc. Int. Conf. Signal Process. Commun. (ICSC)*, Mar. 2015, pp. 183–188.
[76] E. Gandini, M. Ettorre, R. Sauleau, and A. Grbic, "A lumped-element unit cell for beam-forming networks and its application to a miniaturized butler matrix," *IEEE Trans. Microw. Theory Techn.*, vol. 61, no. 4, pp. 1477–1487, Apr. 2013.
[77] C.-W. Wang, T.-G. Ma, and C.-F. Yang, "A new planar artificial transmission line and its applications to a miniaturized butler matrix," *IEEE Trans. Microw. Theory Techn.*, vol. 55, no. 12, pp. 2792–2801, Dec. 2007.
[78] O. Abu Safia, M. Nedil, M. C. E. Yagoub, and W. Yusuf, "Optically transparent compact 4×4 butler matrix for Wi-Fi applications," *Prog. Electromagn. Res. Lett.*, vol. 58, pp. 119–124, 2016.
[79] A. K. Vallappil and M. Rahim, "Metamaterial based compact branch-line coupler with enhanced bandwidth for use in 5G applications," *Appl. Comput. Electromagn. Soc.*, vol. 35, no. 6, p. 15, Jun. 2020.
[80] A. Karimbu Vallappil, M. K. A. Rahim, B. A. Khawaja, and M. N. Iqbal, "Compact metamaterial based 4 × 4 butler matrix with improved bandwidth for 5G applications," *IEEE Access*, vol. 8, pp. 13573–13583, Jan. 2020.
[81] F. Pizarro, D. Ramírez-Gil, A. Algaba-Brazález, L. F. Herrán-Ontanón, and E. Rajo-Iglesias, "Comparison study of 4 × 4 butler matrices in microstrip technologies for ka-band," *Int. J. Electron. Commun.*, vol. 122, Jul. 2020, Art. no. 153248, doi: 10.1016/j.aeue.2020.153248.
[82] I. Messaoudene, H. Youssouf, M. Bilal, M. Belazzoug, and S. Aidel, "Performance improvement of multilayer butler matrix for UWB beamforming antenna," in *Proc. Seminar Detection Syst. Archit. Technol. (DAT)*, 2017, pp. 1–4.
[83] Y. Zhai, X. Fang, K. Ding, and F. He, "Miniaturization design for 8×8 butler matrix based on back-to-back bilayer microstrip," *Int. J. Antennas Propag.*, vol. 2014, pp. 1–7, Dec. 2014. Accessed: Oct. 25, 2017. [Online]. Available: https://www.hindawi.com/journals/ijap/2014/583903/citations/
[84] S. F. Ausordin, S. K. Abdul Rahim, N. Seman, R. Dewan, and B. Sa'ad, "A compact 4×4 butler matrix on double-layer substrate," *Microw. Opt. Technol. Lett.*, vol. 56, no. 1, pp. 223–229, Jan. 2014.
[85] O. M. Haraz and A.-R. Sebak, "Two-layer butterfly-shaped microstrip 4×4 butler matrix for ultra-wideband beam-forming applications," in *Proc. IEEE Int. Conf. Ultra-Wideband (ICUWB)*, Sep. 2013, pp. 1–6.
[86] L. Abdelghani, T. A. Denidni, and M. Nedil, "Design of a new ultra-wideband 4×4 butler matrix for beamforming antenna applications," in *Proc. IEEE Int. Symp. Antennas Propag.*, Jul. 2012, pp. 1–2.
[87] M. Nedil, T. A. Denidni, and L. Talbi, "Novel butler matrix using CPW multilayer technology," *IEEE Trans. Microw. Theory Techn.*, vol. 54, no. 1, pp. 499–507, Jan. 2006.
[88] Y. Kozuki and H. Arai, "Layered butler matrix circuit for vertical multi beam of cellular base station antenna," in *Proc. Int. Symp. Antennas Propag. Conf. Proc.*, Dec. 2014, pp. 561–562.
[89] A. A. M. Ali, N. J. G. Fonseca, F. Coccetti, and H. Aubert, "Design and implementation of two-layer compact wideband butler matrices in SIW technology for ku-band applications," *IEEE Trans. Antennas Propag.*, vol. 59, no. 2, pp. 503–512, Feb. 2011.
[90] A. Corona and M. J. Lancaster, "A high-temperature superconducting butler matrix," *IEEE Trans. Appiled Supercond.*, vol. 13, no. 4, pp. 3867–3872, Dec. 2003.
[91] F. Wu and L. Sun, "Miniaturization of 4×4 butler matrix using high slow-wave factor structure," in *Proc. IEEE 2nd Adv. Inf. Technol., Electron. Autom. Control Conf. (IAEAC)*, Mar. 2017, pp. 1772–1775.
[92] K. Wincza and K. Sachse, "Broadband 4 x 4 Butler matrix in microstrip multilayer technology designed with the use of three-section directional couplers and phase correction networks," *Proc. 18th Int. Conf. Microw., Radar And Wireless Commun.*, vol. 2010, pp. 1–4.
[93] K. Staszek, S. Gruszczynski, and K. Wincza, "Broadband measurements of *S*-parameters with the use of a single 8 × 8 butler matrix," *IEEE Trans. Microw. Theory Techn.*, vol. 62, no. 2, pp. 352–360, Feb. 2014.
[94] S. Karamzadeh, V. Rafii, M. Kartal, and B. S. Virdee, "Compact and broadband 4 × 4 SIW butler matrix with phase and magnitude error reduction," *IEEE Microw. Wireless Compon. Lett.*, vol. 25, no. 12, pp. 772–774, Dec. 2015.
[95] T. Djerafi, N. J. G. Fonseca, and K. Wu, "Design and implementation of a planar 4x4 butler matrix in SIW technology for wideband applications," in *Proc. 40th Eur. Microw. Conf.*, 2010, pp. 910–913.
[96] S. Gruszczynski, K. Wincza, and K. Sachse, "Compact broadband Butler matrix in multilayer technology for integrated multibeam antennas," *Electron. Lett.*, vol. 43, no. 11, pp. 635–636, May 2007.

[97] Y. J. Cheng, C. A. Zhang, and Y. Fan, "Miniaturized multilayer folded substrate integrated waveguide butler matrix," *Prog. Electromagn. Res.*, vol. 21, pp. 45–58, 2011, doi: 10.2528/PIERC11020502.

[98] K. Shafique, B. A. Khawaja, M. D. Khurram, S. M. Sibtain, Y. Siddiqui, M. Mustaqim, H. T. Chattha, and X. Yang, "Energy harvesting using a low-cost rectenna for Internet of Things (IoT) applications," *IEEE Access*, vol. 6, pp. 30932–30941, Jun. 2018.

[99] H. Yu, H. Lee, and H. Jeon, "What is 5G? Emerging 5G mobile services and network requirements," *Sustainability*, vol. 9, no. 10, p. 1848, Oct. 2017.

[100] T. Rappaport, Y. Xing, O. Kanhere, S. Ju, A. Madanayake, S. Mandal, and G. Trichopoulos, "Wireless communications and applications above 100 GHz: Opportunities and challenges for 6G and beyond," *IEEE Access*, 7, pp. 78729–78757, 2019.

[101] K. Shafique, B. A. Khawaja, F. Sabir, S. Qazi, and M. Mustaqim, "Internet of Things (IoT) for next-generation smart systems: A review of current challenges, future trends and prospects for emerging 5G-IoT scenarios," *IEEE Access*, vol. 8, pp. 23022–23040, Feb. 2020.

[102] *5G Millimeter Wave Frequencies and Mobile Networks Technology Whitepaper—Remcom—Articles and Papers*. Accessed: Sep. 24, 2020. [Online]. Available: https://www.remcom.com/articles-and-papers/5g-millimeter-wave-frequencies-and-mobile-networks-technology-whitepaper

ARSHAD KARIMBU VALLAPPIL received the B.Tech. degree in electronics and communication engineering from the University of Calicut, Kerala, India, in 2009, and the M.Tech. degree in electronics engineering from Pondicherry University, Puducherry, India, in 2013. He is currently pursuing the Ph.D. degree in electrical engineering with University Teknologi Malaysia, Malaysia. His research interests are RF and microwave systems, antenna arrays, and beamforming networks.

MOHAMAD KAMAL A. RAHIM (Senior Member, IEEE) was born in Alor Setar, Malaysia, in 1964. He received the B.Eng. degree in electrical and electronic engineering from the University of Strathclyde, U.K., in 1987, the master's degree in engineering from the University of New South Wales, Australia, in 1992, and the Ph.D. degree in the field of wideband active antenna from the University of Birmingham, U.K., in 2003. From 1992 to 1999, he was a Lecturer with the Faculty of Electrical Engineering, Universiti Teknologi Malaysia. He was a Senior Lecturer with the Department of Communication Engineering from 2005 to 2007. He is currently a Professor with Universiti Teknologi Malaysia. His research interests include the design of active and passive antennas, dielectric resonator antennas, microstrip antennas, reflectarray antennas, electromagnetic bandgap, artificial magnetic conductors, left-handed metamaterials, and computer-aided design for antennas.

BILAL A. KHAWAJA (Senior Member, IEEE) received the B.S. degree in computer engineering from the Sir Syed University of Engineering and Technology, Karachi, Pakistan, in 2002, the M.Sc. degree in communication engineering and signal processing from the University of Plymouth, Plymouth, U.K., in 2005, and the Ph.D. degree in electrical engineering from the University of Bristol, Bristol, U.K., in 2010. From 2003 to 2004, he was a Software Engineer with Simcon International (Pvt.) Ltd., Pakistan. From 2010 to 2016, he was an Assistant Professor with the Department of Electronics and Power Engineering, PN-Engineering College, National University of Science and Technology, Karachi. In 2015, he was a Visiting Postdoctoral Researcher with the Lightwave Systems Research Laboratory, Queen's University, Kingston, Canada, involved in the Natural Sciences and Engineering Research Council, Canada CREATE Next Generation Optical Network Project on the characterization and measurements of 25-GHz RF signal generation optical comb sources. He is currently an Associate Professor with the Department of Electrical Engineering, Faculty of Engineering, Islamic University of Madina, Madina, Saudi Arabia. He has authored and coauthored several journals and IEEE proceeding publications. His current research interests include next-generation of millimeter-wave (mm-wave) radio-over-fiber and optical communication systems, mm-wave and THz signal generation mode-locked lasers and RF transceiver design and antennas design/characterization for the Wi-Fi/IoT/UAVs/FANETs/5G systems/UWB wireless body area networks, wireless sensor networks, and millimeter-wave frequency bands. He is an active reviewer for many reputed IEEE journals and letters.

NOOR ASNIZA MURAD (Senior Member, IEEE) received the B.Eng. degree in electrical engineering majoring in telecommunication and the M.Eng. degree from Universiti Teknologi Malaysia (UTM), Malaysia, in 2001 and 2003, respectively, and the Ph.D. degree in electrical and electronic engineering from the University of Birmingham, U.K., in 2011. She joined as a Tutor with the Department of Radio Communication Engineering, Faculty of Electrical Engineering, UTM, and was appointed as a Lecturer in April 2003, where she is currently a Senior Lecturer. Her research interests include antenna design for RF and microwave communication systems, millimeter-wave circuits design, and antenna beamforming.

MOHAMMED GAJIBO MUSTAPHA received the Diploma degree in telecommunication engineering from Multimedia University Melaka in 2009, the degree in electrical/electronic engineering from the University of Sunderland, U.K., in 2013, and the M.Eng. degree in electrical and telecommunication engineering and the Ph.D. degree in the field of meta-material absorbers and reflectors from Universiti Teknologi Malaysia, Malaysia, in 2015 and 2020, respectively.